



OPEN The density histograms-derived computerized integrated index (CII) predicts mortality in idiopathic pulmonary fibrosis

Gaetano Rea¹, Roberta Lieto¹, Dario Bruzzese², Paola Rebecca Iovine³, Annalisa Mazzocca³, Stefano Sanduzzi Zamparelli³ & Marialuisa Bocchino³✉

Quantitative assessment of the extent of radiological alterations in interstitial lung diseases is a promising field of application that goes beyond the limitations of qualitative scoring. Analysis of density histograms, i.e., skewness, kurtosis, and mean lung attenuation, is among the most studied approaches. We recently proposed their integration in a single parameter, the computerized integrated index (CII), to reduce their redundancy. The CII has proven effective in detecting subclinical lung involvement, correlates with lung function/disease activity, and predicts mortality in systemic sclerosis patients. Seventy-three newly diagnosed and therapy-naïve IPF patients (M = 50; median age: 70.2 years) were prospectively enrolled from January 2014 to December 2022, and followed till December 2023. At baseline, all underwent lung function testing and volumetric high resolution chest CT. Density histograms were analyzed with an open-source automatic platform (Slicer 3D) and CII derived by means of Principal Component Analysis, as previously described. During a median follow-up of 5.8 years, 39 (53.4%) subjects died. Median overall survival (OS) was 4.9 years (95% CI 3.7 years-*not estimable*). The CII was significantly associated with OS (HR 0.49; 95% CI 0.35–0.68; $P < 0.001$) and correlated with lung function ($r = 0.41$; 95% CI 0.19 to 0.60; $P < 0.001$ for FVC, and $r = 0.62$; 95% CI 0.44 to 0.75; $P < 0.001$ for DLCO_{sb}). Patients stratification according to CII tertile, showed a consistent reduction in the hazard of death. After adjusting for body mass index, smoking, GAP stage, and anti-fibrotic therapy, the CII preserved a significant association with the hazard of death (HR 0.35; 95% CI 0.2–0.63; $P < 0.001$). CII is a proxy marker of IPF severity worthy of use for prognostication purposes in daily practice.

Keywords Idiopathic pulmonary fibrosis, High resolution chest CT, Density histograms, Computerized integrated index, Mortality

Abbreviations

BMI	Body mass index
CII	Computerized integrated index
DLCO _{sb}	Single-breath lung diffusion capacity for CO
FVC	Forced vital capacity
GAP	Gender-age-physiology
HR	Hazard ratio
HRCT	High resolution computed tomography
ILD	Interstitial lung disease
IPF	Idiopathic pulmonary fibrosis
MLA	Mean lung attenuation
OS	Overall survival
SD	Standard deviation
SSc	Systemic sclerosis

¹Department of Radiology, Monaldi Hospital, Azienda Ospedaliera (AO) dei Colli, Naples, Italy. ²Department of Public Health, Federico II University of Naples, Naples, Italy. ³Respiratory Medicine Unit, Department of Clinical Medicine and Surgery, Monaldi Hospital- AO dei Colli, Federico II University of Naples, Via L. Bianchi, 5, 80131 Naples, Italy. ✉email: marialuisa.bocchino@unina.it

UIP Usual interstitial pneumonia

Idiopathic pulmonary fibrosis (IPF) remains the most aggressive form among interstitial lung diseases (ILDs), being the most frequent entity among those with unknown cause. The original fibrosing imprint differentiates it from all other ILDs whose pathogenesis is attributable to an inflammatory process. The prognosis of patients affected by IPF is severe with a median survival of 3–5 years in untreated cases. The availability of two anti-fibrotic drugs, that is nintedanib and pirfenidone, over the last decade has helped to slow down the evolution of the disease, whose natural course still remains unpredictable to date^{1–3}. Monitoring of the decline of lung function indices continues to be the most widely used prognostic tool both in the setting of clinical trials and in daily practice¹. This custom resulted in the multi-parameter GAP (gender-age-physiology) index that integrates the prognostic value of lung function, that is the forced vital capacity (FVC) and the lung diffusion capacity for CO (DLCO), with the patient's age and gender⁴. While the index is easy to calculate and use, it does not provide any indication about the extent of the disease. The radiological assessment of the IPF patient represents a key element in the diagnostic process, being pathognomonic the association with a usual interstitial pneumonia (UIP) pattern^{1–3}. The individual radiological findings have not only descriptive value, but those associated with the irreversible distortion of the lung parenchyma, such as traction bronchiolectasis and honeycombing, also prognostic. However, the heterogeneity and complexity of distribution of chest CT individual findings have strongly limited the development of objective and reproducible indicators of ready use. In fact, the qualitative evaluation of disease extension, although simple and rapid, is burdened by a not negligible intra- and inter-operator variability^{5–9}. In an attempt to overcome these limitations, different quantitative approaches have been explored over time. Among the first and probably most studied are the three density-based histograms, i.e., skewness (degree of histogram asymmetry), kurtosis (degree of histogram peakedness), and mean lung attenuation (MLA, average global attenuation value of the lung parenchyma). They are easy to measure through the use of free platforms available online and relatively not time consuming. A further strength of these indicators is their proven correlation with both lung function and quality of life in patients with ILD^{7,8,10,11}. In the light of these considerations and with the aim of further simplifying their use on a large scale in clinical practice, we proposed their integration in a single composite index by means of Principal Component Analysis to reduce redundancy. The computerized integrated index (CII) has proven effective in detecting subclinical lung involvement in patients affected by systemic sclerosis (SSc) visually-free from ILD at chest CT. Also, the CII correlated with lung function and disease activity, as assessed by immune-inflammatory mediators¹². These observations represented the starting point for further studies that led to the validation of the CII in two independent European cohorts of SSc-related ILD patients, with an additional association with mortality. The performance and prognostication value of the CII in the IPF patient has not been explored to date¹³.

Given this background, the purpose of our study was to assess the mortality predictive value of the CII in a prospective cohort of patients with IPF enrolled at a tertiary reference center at the time of first diagnosis and followed-up over a 10-year observation period.

Methods

Patients enrollment and clinical assessment

The study population included newly diagnosed and therapy-free adult (>18-years) patients with IPF prospectively referring to our clinic from January 2014 to December 2022. Diagnosis of IPF was made according to international guidelines at the time of patient assessment^{1–3}. Exclusion criteria were diagnosis of lung diseases other than IPF, acute exacerbation in the first four weeks before the study visit, and coexistence of any neoplasm at the time of IPF diagnosis. Patients with a follow-up of less than 1-year were not included in final analysis (end of the observation period: December 31st, 2023). At baseline, all study participants underwent lung function assessment including spirometry, lung volume measurement, and single-breath DLCO (DLCO_{sb}), according to the American Thoracic Society/European Respiratory Society criteria^{14–17}. The GAP index was calculated as previously reported⁴. Data of interest for the study were collected anonymously into a dedicated database. The study was performed according to the amended Declaration of Helsinki. The local Institutional Ethics Committee of the approved the study (Azienda Ospedaliera dei Colli- protocol number 407/2014) and all participants provided written informed consent.

Chest CT imaging and computerized integrated index calculation

Volumetric high resolution computed tomography (HRCT) of the chest was obtained with a 64-slice multi-detector CT scanner (MDCT 64, General Electric Medical System, Milwaukee, WI). Patients were in the supine position, at full inspiration. Scan parameters were 120 kV and 80 mAs, by applying the smallest field of view according to the patient body habitus. Matrix size was 512×512 pixels; images were reconstructed with a 1/1.25 mm slice thickness using the bone filters. The whole lung volume was processed and stored on a picture archiving and communication system (PACS) for post-processing evaluation. The lung parenchyma was analyzed by two radiologists experts in interstitial lung disease (GR and RL, with a 20 and 5 years of experience, respectively) with a window width of 1.600 Hounsfield Units (HU) and –600 HU. The definition of the chest CT pattern at disease presentation has been retrospectively re-analyzed, according to the latest international guidelines to make the nomenclature uniform. MLA, skewness, and kurtosis were calculated using an automated free open-source software for digital image processing (Slicer 3D)^{18–20}. Representative examples of visual and digital image processing are shown in Fig. 1. Average values of MLA, skewness, and kurtosis were generated and used to calculate the computerized integrated index (CII), by means of Principal Component Analysis (PCA), as previously described¹².

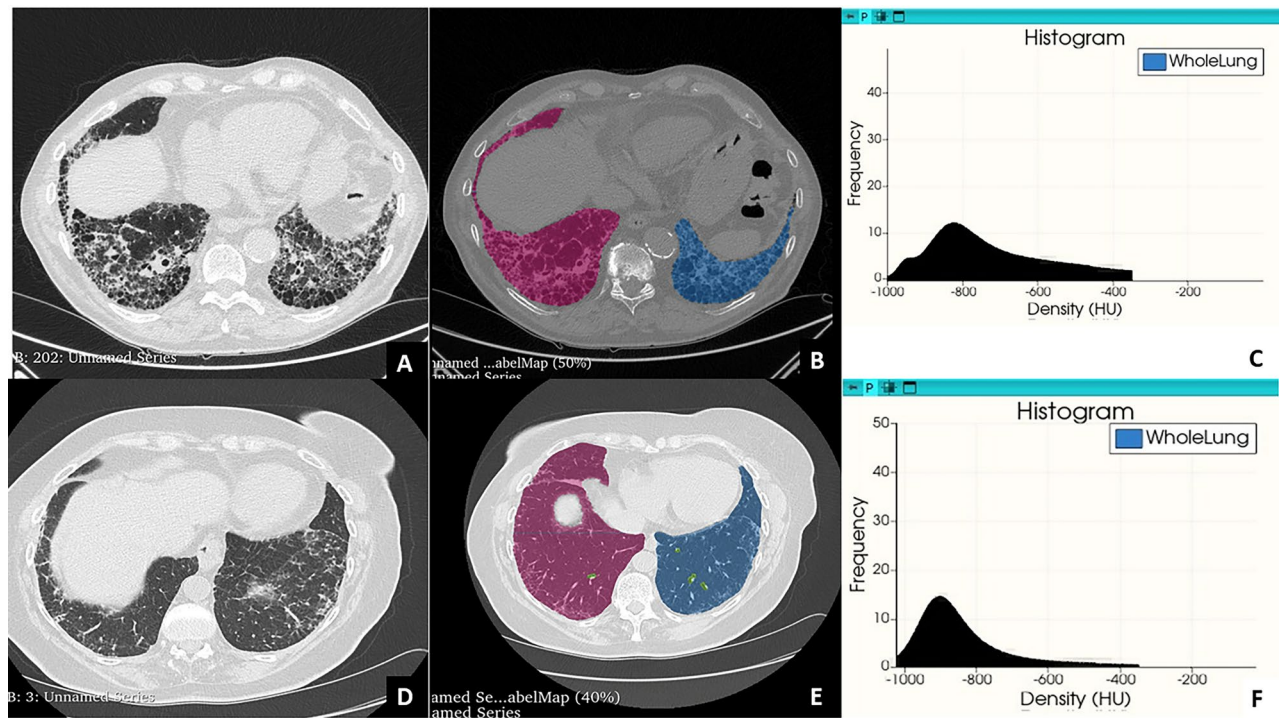


Fig. 1. High resolution chest CT findings in a patient with a usual interstitial pneumonia (UIP) pattern (A) and automated color-coded lung segmentation in a single representative slice (B). Representative histogram of the whole density of the lungs (C). High resolution chest CT findings in a patient with a probable usual UIP pattern (D) and automated color-coded segmentation in a single representative slice (E). Representative histogram of the whole density of the lungs (F).

Statistical analysis

Standard descriptive statistics were used to describe the cohort: mean \pm standard deviation (SD) (range) or median [25th; 75th percentile] (range) in case of numerical variables and absolute frequency with percentages for categorical factors. Correlation between CII and functional respiratory parameters was assessed using the Pearson correlation coefficient.

Overall Survival (OS) was defined as the time from the IPF diagnosis to all-cause-death. For patients who were alive at the end of the observational period, OS was censored on 31th December 2023. Median OS was estimated using the Kaplan–Meier method and the association between CII (both as continuous variable and as categorical factor based on tertiles) and mortality was explored using univariate and multivariable Cox regression models after assessing the proportional hazard assumption adding an interaction with time in the models. Results of Cox models were expressed as Hazard ratios (HRs) with 95% Confidence Intervals (95% CI).

Statistical analyses were performed using R (version 4.0.2, R Foundation for Statistical Computing, Vienna, Austria).

Results

A total of 73 subjects were enrolled in our study cohort (Fig. 2). Demographics and clinical characteristics of participants are reported in Table 1. Median age at IPF diagnosis was 70.2 years, and the majority of cases (68.5%) were males. Most of the patients had a mild/moderate IPF according to the GAP disease staging index. Systemic arterial hypertension was the most prevalent comorbidity (52%). Almost half of them presented with chest CT lung alterations compatible with a UIP pattern (50.7%), according to the last guideline document. Sixty-one (82.2%) patients were treated with available anti-fibrotic drugs, that is nintedanib and pirfenidone. The remaining 12 cases refused treatment or were not eligible. During a median follow up of 5.9 years, 39 (53.4%) subjects died with 26 deaths due to disease progression. Death occurred due to acute exacerbation in 4 cases, to *ictus cerebri* (n=4), pulmonary embolism (n=2), and cancer (lung and pancreas) in further three cases. Median overall survival was equal to 4.9 years (95% CI 3.7 years to *Not Estimable*). As expected, GAP index was a significant predictor of mortality (log-rank $P=0.001$) with a reduced survival in patients with higher stage while the different treatment regimens (nintedanib, pirfenidone or no treatment) did not impact on mortality (log rank $P=0.160$) (Fig. 3).

Mean (\pm SD) of the three components of the CII (i.e. skewness, kurtosis and MLA) are reported in Table 2. CII index significantly correlated with lung function parameters (Fig. 4), in particular with FVC ($r=0.41$; 95% CI 0.19 to 0.60; $P<0.001$), total lung capacity ($r=0.38$; 95% CI 0.12 to 0.60; $P=0.006$) and DLCO_{sb} ($r=0.62$; 95% CI 0.44 to 0.75; $P<0.001$).

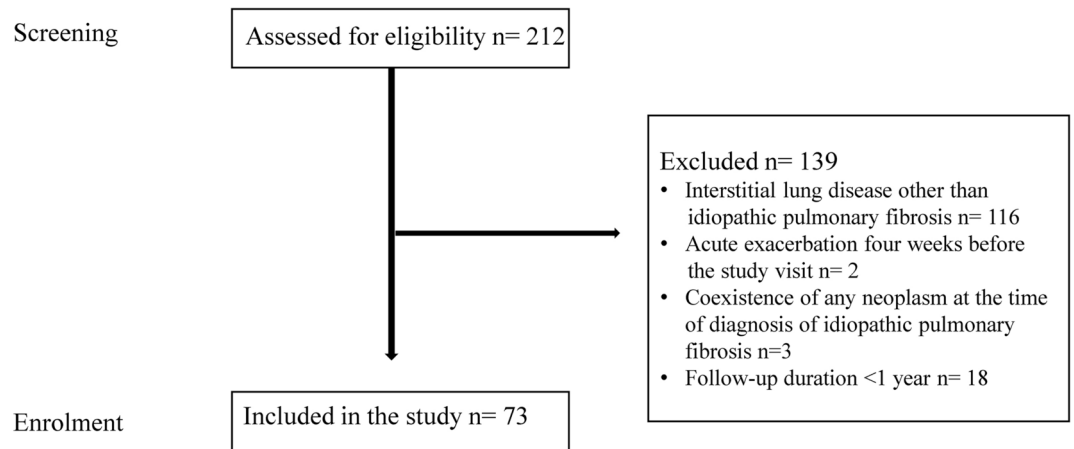


Fig. 2. Flow chart showing the selection of the study population.

The CII was significantly associated with the OS with, approximately, a half reduction in the hazard of death for every increase in the index (HR 0.49; 95% CI 0.35 to 0.69; $P < 0.001$). When patients were stratified according to the CII tertiles, a consistent reduction in the hazard of death was observed (Fig. 5). Median OS of patients in the lower and medium tertile of CII were, respectively, 2.6 years (95% CI 1.6 to 4.0) and 5.2 years (95% CI 2.7 to *Not estimable*), while median OS was not reached in the upper CII tertile.

In the subset of treated patients, after adjusting for body mass index (BMI), smoking habit, GAP stage, UIP pattern, and therapy (pirfenidone vs. nintedanib), the CII preserved a significant association with the hazard of death (HR 0.39; 95% CI 0.21 to 0.71; $P = 0.002$), and the only remaining significant predictor of mortality was disease severity according to GAP stage (Table 3).

Discussion

To the best of our knowledge, this is the first prospective study that evaluated the performance of the computerized integrated index as a predictor of mortality in patients with IPF. The CII was significantly associated with the overall survival of 73 newly diagnosed patients with IPF over a 10-year observation period, with a median follow-up of 5.9 years. The lower the CII, the greater was the lung involvement with, approximately, a half reduction in the hazard of death for every increase in the index (HR 0.49; 95% CI 0.35 to 0.69; $P < 0.001$).

Exceeding the well-known limits of visual/qualitative evaluation (i.e., low sensitivity, inter- and intra-operator variability), chest CT quantitative analysis of fibrotic interstitial lung alterations is a field of application of current interest. Numerous efforts have been made over the years, however, the need for a biomarker that is reliable, easy to use, and widely available, still remains pending. With the ambition to identify a parameter that could meet these requirements, in 2019 we first described the CII in a cohort of 83 patients affected by SSc. The CII was incorporating CT density histogram metrics (e.g., skewness, kurtosis and mean lung attenuation) by means of Principal Component Analysis, to reduce their redundancy. At that time, we chose density-based histograms as they were the most widely used among various quantitative tools, as easy to measure through free and not time consuming platforms available online accessible to all. The CII strongly differentiated SSc patients with and without ILD, with an excellent reproducibility. Also, the CII correlated with lung function and disease activity, and was sufficiently sensitive to capture early lung density changes in visually ILD-free patients¹². Given this promising potential, the CII has been validated in two independent cohorts of patients affected by SSc with ILD, and associated with mortality in the same clinical setting¹³.

As previously reported for its individual components⁸, the CII correlated also in our study participants with lung function parameters. Among these, FVC remains the measurement of wider use in real-life practice for predicting disease progression, due to its simplicity of execution and good reproducibility. For these same reasons, it remains also the main outcome in experimental drug clinical trials²¹. However, as FVC is not a validated surrogate of mortality, in 2012 was introduced the GAP multi-parametric index (which integrates age, gender, and DLCO, apart from FVC) that up to date represents the outcome predictor most widely used in daily practice²². Interestingly, in our series, after adjusting for BMI, smoking habit, GAP stage, UIP pattern, and anti-fibrotic therapy, the CII preserved a significant association with the hazard of death (HR 0.39; 95% CI 0.21 to 0.71; $P = 0.002$). Disease severity, according to GAP staging, was the only remaining significant predictor of mortality. The UIP vs. the UIP probable pattern on chest CT imaging was not predictive of outcome suggesting visual differentiation not useful for prognostication purposes. This was not so surprising as the UIP (already identified as “definite”) and probable UIP patterns are similarly representative of the irreversible fibrotic distortion of the lung parenchyma, with traction bronchiolectasis and honeycombing being both established bad prognosis chest CT findings³. Finally, in agreement with our previous observations²³, we found no difference in terms of survival between IPF patients, either untreated or treated with pirfenidone or nintedanib.

From the methodological point of view, the present study differs from our preliminary experience. Its strength is represented by the use of an image processing platform (Slicer 3D) served by a free open-source software which is easy to use with minimal intervention by the operator. It allows the automated lung segmentation along

Study participants (N)	73
Gender	
Female	23 (31.5)
Male	50 (68.5)
Age (years) at diagnosis	70.2 [66.7; 74] (38.8–85.3)
BMI (kg/m ²)	27.6 [25.6; 30.4] (16.4–39.8)
Smoking habit	
Never	16 (21.9)
Former smoker	57 (78.1)
Current smoker	0
Comorbidities	
Systemic arterial hypertension	39 (53.4)
Type II diabetes	15 (20.5)
Cardio-vascular diseases	17 (23.3)
Gastro-esophageal reflux	27 (36.9)
Obstructive sleep apnea	24 (32.8)
Lung function	
FVC (% pred)	75.5 ± 25.9 (32–144)
TLC (% pred)	63.4 ± 15.2 (37–90)
DLCO _{sb} (% pred)	50 ± 15.5 (16–92)
GAP stage	
Stage 1	26 (41.3)
Stage 2	29 (46)
Stage 3	8 (12.7)
Chest CT pattern	
UIP	37 (50.7)
UIP probable	36 (49.3)
Antifibrotic-therapy	
Nintedanib	28 (38.3)
Pirfenidone	33 (45.2)
None	12 (16.4)

Table 1. Demographics and clinical features of the study population. Data are expressed as No. (%), or median [IQR25–IQR75] (range), or mean ± SD (range). BMI, body mass index; FVC, forced vital capacity; TLC, total lung capacity; DLCO_{sb}, single-breath diffusion lung capacity for CO; GAP, gender-age-physiology; IQR, interquartile range; SD, standard deviation; UIP, usual interstitial pneumonia.

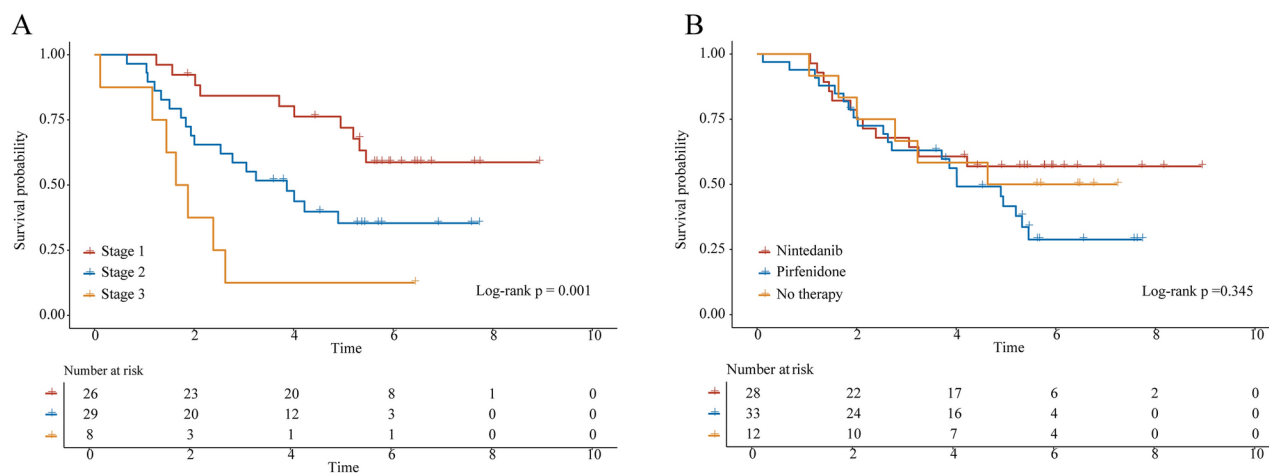


Fig. 3. Overall survival of patients with idiopathic pulmonary fibrosis according to GAP (gender-age-physiology) stage (A) and treatment regimen (B).

Parameter	Value
Skewness	1.6 ± 0.6 (0.4–3.1)
Kurtosis	5.7 ± 2.6 (2–14.4)
Mean lung attenuation (HU)	-705.8 ± 85.3 (-843.8 to -489.1)

Table 2. Automated estimates of chest CT- based density-histograms by digital image processing in the study population. Data are expressed as mean ± SD (range). HU, Hounsfield Unit. Skewness and kurtosis are descriptive statistical parameters (pure numbers) respectively indicative of the degree of histogram asymmetry and peakedness.

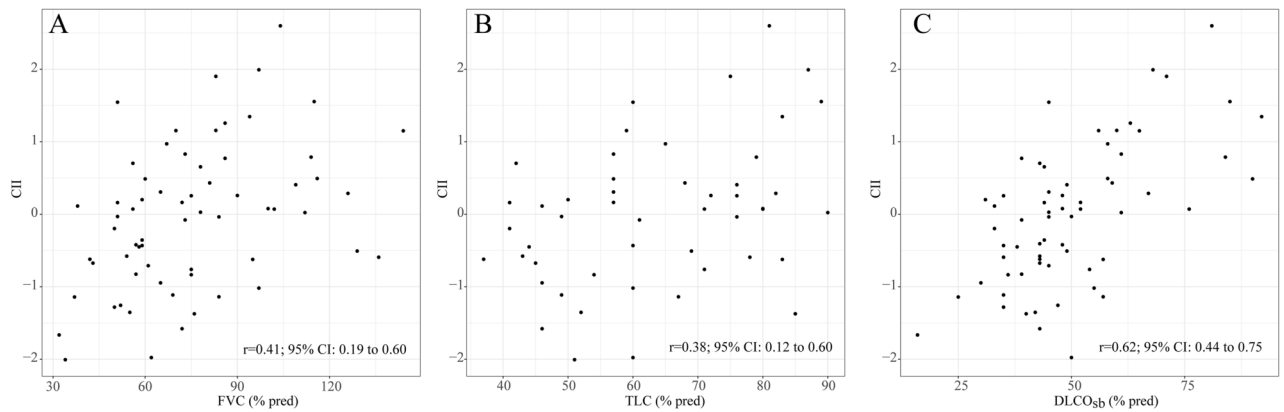


Fig. 4. Scatter plot showing correlation between the computerized integrated index (CII) and parameters of lung function. (A) Forced vital capacity (FVC) % of predicted; (B) Total lung capacity (TLC) % of predicted; (C) Single-breath diffusion lung capacity for CO (DLCO_{sb}) % of predicted.

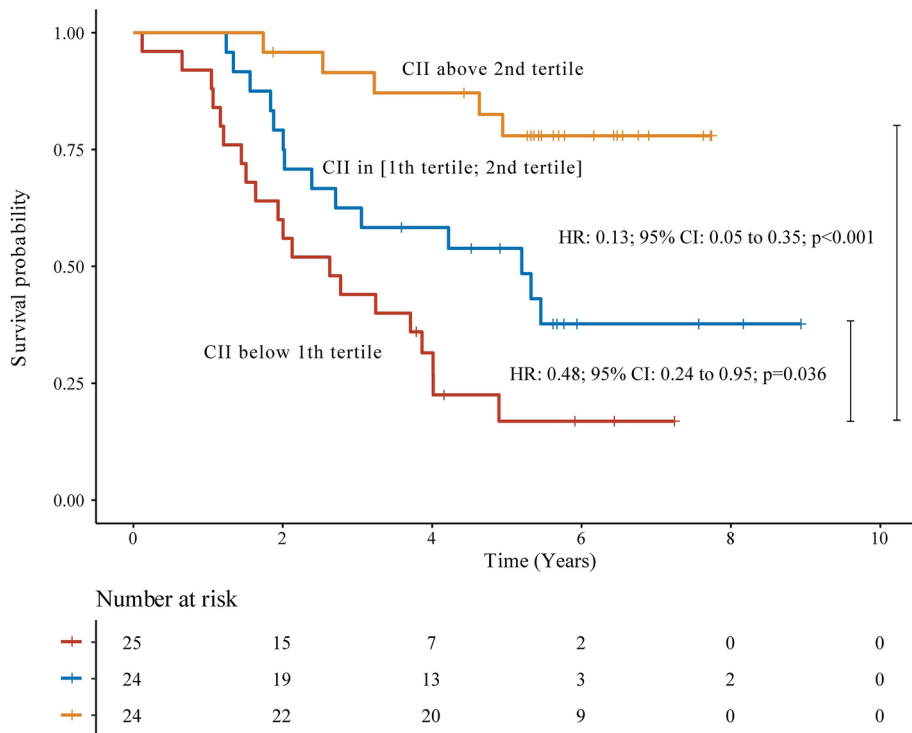


Fig. 5. Overall survival of patients with idiopathic pulmonary fibrosis treated with anti-fibrotic drugs according to the computerized integrated index (CII).

Parameter	HR (95% CI)	P value
CII	0.39 (0.21–0.71)	0.002
BMI	1 (0.93–1.08)	0.948
Smoking (never ref.)	1.98 (0.75–5.27)	0.169
GAP (Stage 1 ref.)		
Stage 2	1.39 (0.54–3.55)	0.493
Stage 3	6.61 (1.9–23.03)	0.003
UIP pattern (definite ref.)	0.56 (0.23–1.35)	0.197
Anti-fibrotic therapy (pirfenidone ref.)	1.09 (0.45–2.61)	0.848

Table 3. Predictors of mortality in the sub-cohort of patients with idiopathic pulmonary fibrosis treated with anti-fibrotic drugs. CII, computerized integrated index; BMI, body mass index; CI, confidence interval; GAP, gender-age-physiology; UIP, usual interstitial pneumonia. Statistically significant data are reported in bold.

with the generation of 3D models with images in colorimetric scale for a better visual representation. Artificial intelligence (AI)-based segmentation indeed eliminates human variability in contour delineation, minimizes discrepancies between observers, and significantly reduces the evaluation time, for a total duration of 3–10 min per chest CT^{24,25}. These advantages not only eliminate the need to prove the reproducibility of measurements, but are also translated into the possibility of application of the process in clinical practice, even in those contexts where the radiologist's expertise is lacking²⁶.

There is no doubt that our study has some limitations. The first is represented by the sample size which is representative of a single center. Another weakness is the lack of complete data of lung function monitoring during the study period. Unfortunately, the pandemic due to Severe Acute Respiratory Syndrome-Coronavirus-2 infection has imposed restrictive measures for almost two years that have interrupted the continuity of care of these patients with data being missing in a not negligible number of cases. This information would have been useful to evaluate the predictive value of the CII on lung function decline over the years. Another information worthy of study and that could represent the starting point for future efforts is the concomitant chest CT monitoring over time in order to identify those changes of the CII with a potential prognostic value. This aspect could be even of a wider use for its inclusion in the definition criteria of progression of fibrotic interstitial lung diseases, including both IPF and those other than IPF. In this sense, the CII could have an impact both in the design of clinical trials to come as a measure of outcome and for the definition of the timing of initiation of current anti-fibrotic therapies. Last but not least, there are certainly additional software, either free or paid, maybe even more efficient than the one we used, and likely more will be available in the years to come. In our opinion, this is not exactly a limit of the study, but, on the contrary, an incentive to improve the performance of quantitative analysis in the service of clinical and diagnostic needs.

Conclusion

We first reported that the computerized integrated index is an independent predictor of mortality in patients affected by IPF. The CII is an easy to calculate, objective and reproducible biomarker whose methodological standardization in larger cohorts will help to follow up its promising application in the field of pulmonary fibrosis. It is likely that the availability of an application, which would allow its rapid calculation on a large scale, could facilitate its dissemination in clinical practice even in those settings without a specific radiological competence.

Data availability

The data that support the findings of this study are not openly available due to reasons of sensitivity and are available from the corresponding author upon reasonable request.

Received: 17 June 2024; Accepted: 21 October 2024

Published online: 28 December 2024

References

- Raghu, G. et al. An official ATS/ERS/JRS/ALAT statement: Idiopathic pulmonary fibrosis: Evidence-based guidelines for diagnosis and management. *Am. J. Respir. Crit. Care Med.* **183**, 788–824 (2011).
- Raghu, G. et al. Diagnosis of idiopathic pulmonary fibrosis. An official ATS/ERS/JRS/ALAT clinical practice guideline. *Am. J. Respir. Crit. Care Med.* **198**, e44–e68 (2018).
- Raghu, G. et al. Idiopathic pulmonary fibrosis (an update) and progressive pulmonary fibrosis in adults: An official ATS/ERS/JRS/ALAT clinical practice guideline. *Am. J. Respir. Crit. Care Med.* **205**, e18–e47 (2022).
- Ley, B. et al. A multidimensional index and staging system for idiopathic pulmonary fibrosis. *Ann. Intern. Med.* **156**, 684–691 (2012).
- Kazerooni, E. A. et al. Thin-section CT obtained at 10-mm increments versus limited three-level thin-section CT for idiopathic pulmonary fibrosis: correlation with pathologic scoring. *AJR Am. J. Roentgenol.* **169**, 977–983 (1997).
- Goh, N. S. et al. Interstitial lung disease in systemic sclerosis: A simple staging system. *Am. J. Respir. Crit. Care Med.* **177**, 1248–1254 (2008).
- Best, A. C. et al. Quantitative CT indexes in idiopathic pulmonary fibrosis: Relationship with physiologic impairment. *Radiology* **228**, 407–414 (2003).

8. Rea, G. et al. Comparative analysis of density histograms and visual scores in incremental and volumetric high-resolution computed tomography of the chest in idiopathic pulmonary fibrosis patients. *Radiol. Med.* **126**, 599–607 (2021).
9. Jacob, J. et al. Automated quantitative computed tomography versus visual computed tomography scoring in idiopathic pulmonary fibrosis: Validation against pulmonary function. *J. Thorac. Imaging* **31**, 304–311 (2016).
10. Sverzellati, N. et al. Evaluation of quantitative CT indexes in idiopathic interstitial pneumonitis using a low-dose technique. *Eur. J. Radiol.* **56**, 370–375 (2005).
11. Camiciottoli, G. et al. Lung CT densitometry in systemic sclerosis: Correlation with lung function, exercise testing, and quality of life. *Chest* **131**, 672–681 (2007).
12. Bocchino, M. et al. Performance of a new quantitative computed tomography index for interstitial lung disease assessment in systemic sclerosis. *Sci. Rep.* **9**, 9468 (2019).
13. Bruni, C. et al. Histogram-based densitometry index to assess the severity of interstitial lung disease in systemic sclerosis in standard and low-dose computed tomography. *J. Rheumatol.* **51**, 270–276 (2024).
14. Wanger, J. et al. Standardisation of the measurement of lung volumes. *Eur. Respir. J.* **26**, 511–522 (2005).
15. Miller, M. R. et al. Standardisation of spirometry. *Eur. Respir. J.* **26**, 319–338 (2005).
16. Graham, B. L. et al. Standardization of spirometry 2019 update. An official American thoracic society and European respiratory society technical statement. *Am. J. Respir. Crit. Care Med.* **200**, e70–e88 (2019).
17. Stanojevic, S. et al. ERS/ATS technical standard on interpretive strategies for routine lung function tests. *Eur. Respir. J.* **60**, 2101499 (2022).
18. Cheng, G. Z. et al. Three-dimensional printing and 3D Slicer: Powerful tools in understanding and treating structural lung disease. *Chest* **149**, 1136–1142 (2016).
19. Fedorov, A. et al. 3D slicer as an image computing platform for the quantitative imaging network. *Magn. Reson. Imaging* **30**, 1323–1341 (2012).
20. Palmucci, S. et al. Histogram-based analysis in progressive pulmonary fibrosis: Relationships between pulmonary functional tests and HRCT indexes. *Br. J. Radiol.* **96**, 20221160 (2023).
21. Raghu, G. et al. Idiopathic pulmonary fibrosis: Clinically meaningful primary endpoints in phase 3 clinical trials. *Am. J. Respir. Crit. Care Med.* **185**, 1044–1048 (2012).
22. Ley, B. & Collard, H. R. Risk prediction in idiopathic pulmonary fibrosis. *Am. J. Respir. Crit. Care Med.* **185**, 6–7 (2012).
23. Bocchino, M. et al. Disease stage-related survival in idiopathic pulmonary fibrosis patients treated with nintedanib and pirfenidone: An exploratory study. *Respir. Med. Res.* **84**, 101013 (2023).
24. Zhang, Y., Feng, H., Zhao, Y. & Zhang, S. Exploring the application of the artificial-intelligence-integrated platform 3D slicer in medical imaging education. *Diagnostics (Basel)* **14**, 146 (2024).
25. Risoli, C. et al. Different lung parenchyma quantification using dissimilar segmentation software: A multi-center study for COVID-19 patients. *Diagnostics (Basel)* **12**, 1501 (2022).
26. Thillai, M. et al. Deep learning-based segmentation of CT scans predicts disease progression and mortality in IPF. *Am. J. Respir. Crit. Care Med.* **210**(4), 465 (2024).

Author contributions

On behalf of all authors, the corresponding author affirms that this manuscript is an honest, accurate, and transparent account of the study being reported. G.R. and R.L.: data collection, data analysis, and interpretation; D.B.: statistical analysis and writing; P.R.I., A.M. and S.S.Z.: data collection and data analysis; M.B.: study design, data interpretation and writing of the manuscript. All authors edited and approved the manuscript.

Funding

None.

Declarations

Competing interests

The authors declare no competing interests.

Ethics approval and consent to participate

All patients completed informed consent forms, and the study was approved by the Local Ethics Committee (approval number protocol number 407/2014). The study was conducted in accordance with the Declaration of Helsinki.

Consent for publication

All participants provided written informed consent.

Additional information

Correspondence and requests for materials should be addressed to M.B.

Reprints and permissions information is available at www.nature.com/reprints.

Publisher's note Springer Nature remains neutral with regard to jurisdictional claims in published maps and institutional affiliations.

Open Access This article is licensed under a Creative Commons Attribution-NonCommercial-NoDerivatives 4.0 International License, which permits any non-commercial use, sharing, distribution and reproduction in any medium or format, as long as you give appropriate credit to the original author(s) and the source, provide a link to the Creative Commons licence, and indicate if you modified the licensed material. You do not have permission under this licence to share adapted material derived from this article or parts of it. The images or other third party material in this article are included in the article's Creative Commons licence, unless indicated otherwise in a credit line to the material. If material is not included in the article's Creative Commons licence and your intended use is not permitted by statutory regulation or exceeds the permitted use, you will need to obtain permission directly from the copyright holder. To view a copy of this licence, visit <http://creativecommons.org/licenses/by-nc-nd/4.0/>.

© The Author(s) 2024